EarlyView publication on www.interscience.wiley.com
(issue and page numbers not yet assigned;
citable using Digital Object Identifier – **DOI**)

Phys. Status Solidi A, 1–6 (2010) / **DOI** 10.1002/pssa.201000008

physica status solidi a
www.pss-a.com
applications and materials science

Detailed study of superconductivity in nanostructured nanocrystalline boron doped diamond thin films

Soumen Mandal[*,1], Cécile Naud[1], Oliver A. Williams[2], Étienne Bustarret[1], Franck Omnès[1], Pierre Rodière[1], Tristan Meunier[1], Laurent Saminadayar[1,3], and Christopher Bäuerle[1]

[1] Institut Néel, CNRS and Université Joseph Fourier, 38042 Grenoble, France
[2] Fraunhofer Institut Angewandte Festkörperphysik, Tullastraße 72, 79108 Freiburg, Germany
[3] Institut Universitaire de France, 103 Boulevard Saint-Michel, 75005 Paris, France

Received 23 February 2010, revised 19 May 2010, accepted 25 May 2010
Published online 00 Month 2010

Keywords XXXX[Q1]

* Corresponding author: e-mail soumen.mandal@grenoble.cnrs.fr; soumen.mandal@gmail.com, Phone: +33-476889060, Fax: +33-456387089

In this paper, we report on the transport properties of nanostructured boron doped diamond thin films. The nanostructures made from polycrystalline boron doped diamond show clear evidence of superconductivity with critical temperatures in the Kelvin range and critical field in the Tesla range. Such robust superconducting properties in these superhard materials make them promising candidates for superconducting nanoelectromechanical systems.

1 Introduction The huge interest seen in the special class of superconducting materials belonging to the covalent metals started with the discovery of superconductivity in MgB_2 [1]. Ekimov et al. [2] in 2004 reported the superconducting properties of boron doped diamond for the first time. This led to the study of superhard superconducting materials [3, 4]. Apart from the mechanism of superconductivity in these systems, which remain largely unexplored, the very high Young's modulus of boron doped diamond makes it a front runner for making nanoelectro mechanical systems (NEMS) of exceptional high quality factor. Before realizing any NEMS made from boron doped diamond it is, however, essential to prove that both the qualities of this system, i.e. superconductivity [5–7] and mechanical properties [8], are preserved when nanocrystalline layers grown on non-diamond substrate are nanopatterned. Earlier studies in this system have concentrated their attention towards the bulk properties of this system. Hence, it is quite essential to investigate the properties of nanostructured boron doped diamond.

In this paper, a comprehensive study of nanostructured superconducting polycrystalline diamond films is presented. It is shown that these nanostructures have superconducting critical parameters like transition temperature and critical field comparable to that of bulk materials.

2 Experimental The nanocrystalline boron-doped diamond was obtained by chemical vapour deposition on a silicon oxide wafer. Before depositing the thin films, the wafers were cleaned with $NH_3OH/H_2O_2/H_2O$ (1:1:5) solution at 75 °C for 10 min, and rinsed in pure DI water in an ultrasonic bath. Nucleation enhancement on wafers was achieved by seeding the wafer with diamond nanoparticles from an aqueous colloid of monodisperse diamond particles known to have sizes less than 7 nm in solution as confirmed by dynamic light scattering [9, 10]. Atomic force microscope (AFM) measurements have shown this technique to result in uniform nucleation densities far in excess of 10^{11} cm^{-2}. Diamond growth was then performed by microwave plasma enhanced chemical vapour deposition (MPCVD) from 4% CH_4 diluted in H_2 with additional boron from a trimethylboron gas source. A microwave power of 3000 W at 60 mbar, was used with substrate temperature being around 800 °C as monitored *in situ* with a bichromatic pyrometer.

The nanostructures were made using electron beam lithography technique. In Fig. 1, the lithography process is

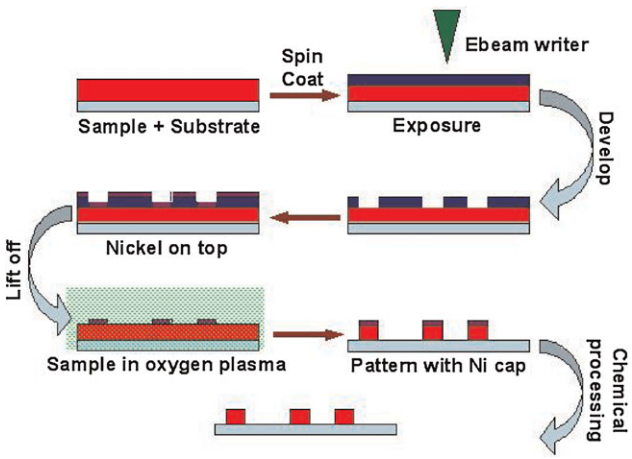

Figure 1 (online colour at: www.pss-a.com) Schematics of the nanofabrication process.

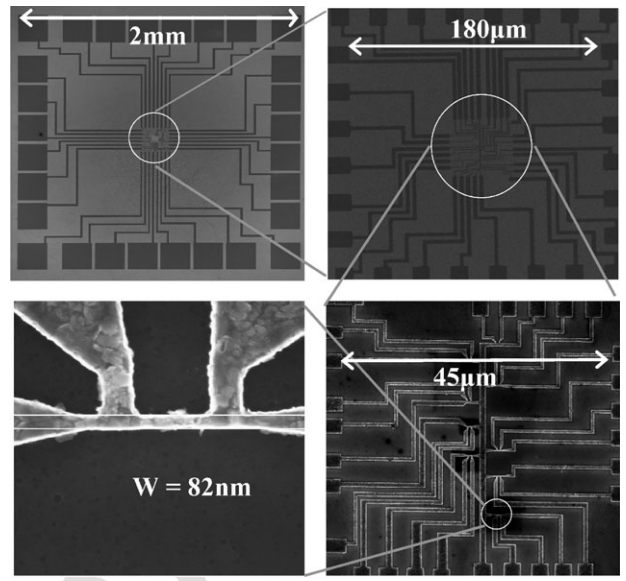

Figure 2 The SEM images of a typical microcircuit fabricated by electron beam lithography.

shown. The wafer was spin coated with 4% polymethylmethacrylate (PMMA) to form a 250 nm thick layer which was prebaked at 180 °C for 5 min. This PMMA layer was exposed to electron beam with a dose of 360 μC cm^{-2} for an acceleration voltage of 20 kV. For the development of the exposed wafer, the wafer was dipped in 1:3 solution of methyl isobutyl ketone (MIBK) and isopropyl alcohol (IPA) for 1 min. A thin layer of nickel (65 nm) was then deposited and patterned using a standard electron-gun evaporator and lift-off technique. This was followed by plasma etching of diamond structures using electron cyclotron resonance oxygen plasma [11] and a −27 V dc bias for ≈8 min. This leads to an etching rate of ≈40 nm/min. The nickel layer acted as a mask in this process. The nickel layer was removed using $FeCl_3$ solution and ohmic contacts were then obtained by an evaporation of metals (Ti–Au).

In Fig. 2, a typical microcircuit fabricated by electron beam lithography technique is shown. The bottom left panel in the figure shows the picture of the line with the smallest width ≈80 nm, which is ≈500 nm long and ≈300 nm thick. Note that in this case the aspect ratio is as high as ∼1:3, the anisotropy of the plasma etching allowing to pattern one single grain. The top and bottom right panels are blow up of $200 \times 200\ \mu m^2$ and $50 \times 50\ \mu m^2$ area in the centre of the microcircuit, respectively.

3 Results and discussion In Fig. 3, the resistance of an unpatterned thin film as a function of temperature is shown. Four silver paste electrical contacts were deposited on the surface of as-grown layer for this measurement. A standard ac lock-in technique with a very low current injection of 1 μA was used for this measurement. The data clearly show a superconducting transition with a zero resistance at ≈3.5 K. The width of the transition is quite large, typically 0.7 K with a 10–90% of the onset resistance criterion. In the inset of the same figure a scanning electron microscope (SEM) picture of the sample with grains of typical size ≈250 nm, for a film thickness of ≈300 nm is shown. The large width of transition seen in the resistivity data is attributed to the distribution of the grain sizes across the sample.

In Fig. 4a and b, the current–voltage characteristic (V–I curve) and the calculated differential resistance for a 350 nm wide and 500 nm long wire is shown. The inset in the panel (a) shows the critical temperature of a few representative wires of varying widths. These measurements were performed in both a ^{3}He and a ^{3}He/^{4}He dilution refrigerators. The current through the sample for these measurements were 100 nA for the 500 nm wide wire and 10 nA for the rest of the

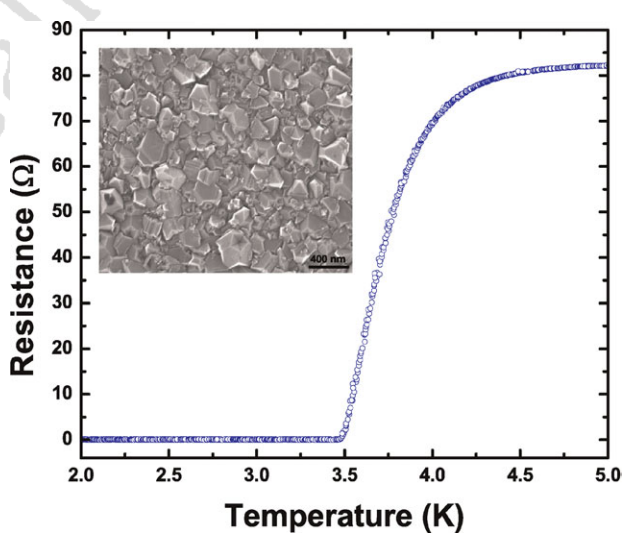

Figure 3 (online colour at: www.pss-a.com) Superconducting resistive transition in a boron-doped diamond thin film. The inset is a SEM image of the surface of the sample, consisting of grains of typically ≈250 nm.

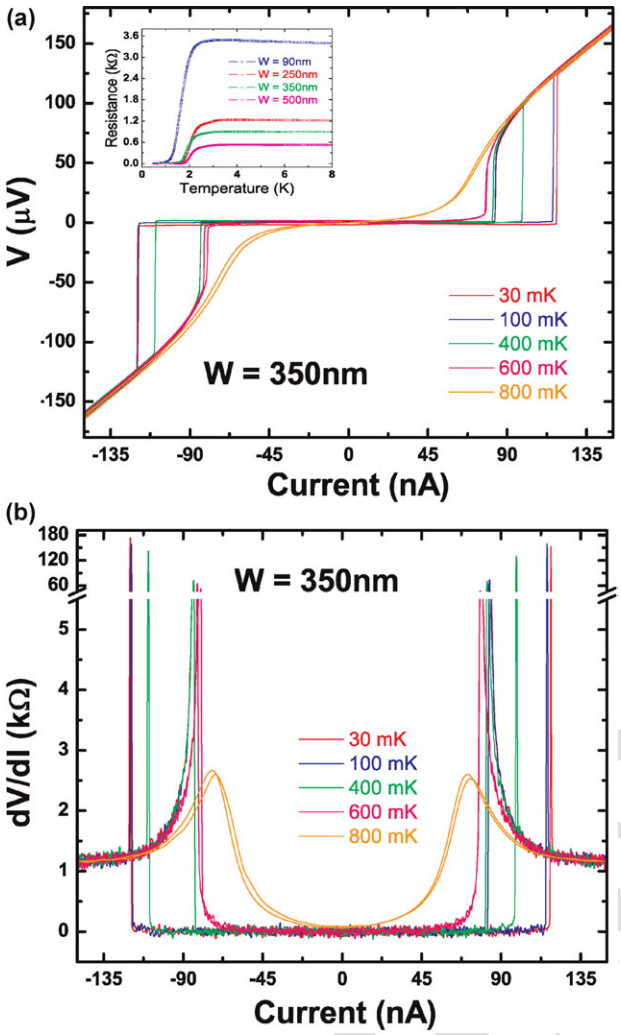

Figure 4 (online colour at: www.pss-a.com) (a) Voltage–current (*V–I*) characteristic of a 350 nm wide wire at different temperatures. The *V–I* curves are hysteretic due to thermal effect (Joule heating). The inset shows the *R* versus *T* curves for four representative wires. (b) Differential resistance extracted from the *V–I* curves. The resistance goes to zero when the wire is in its superconducting state.

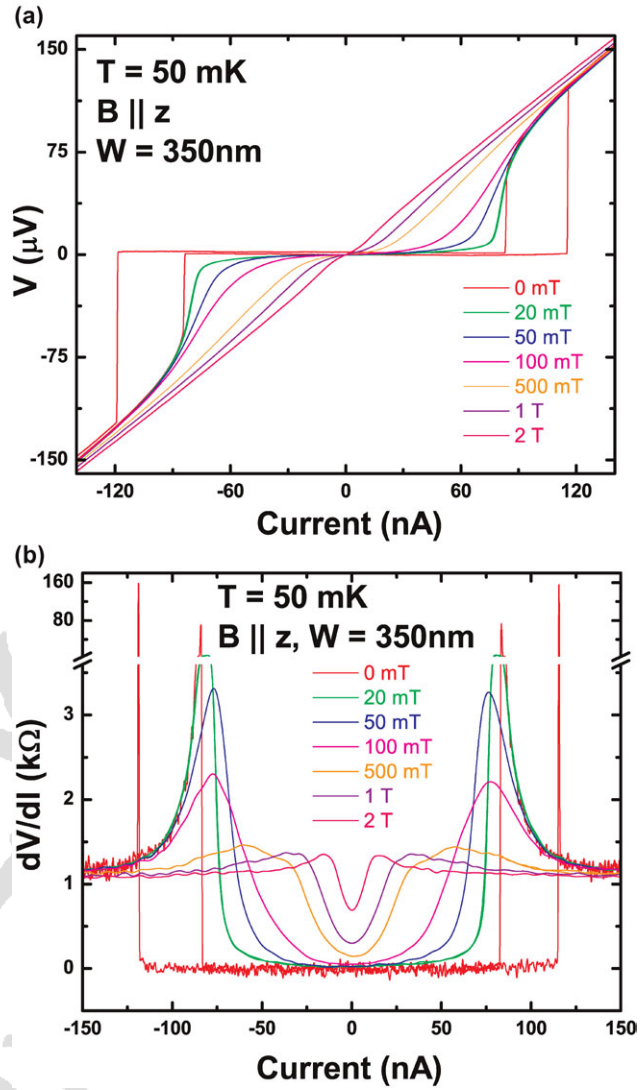

Figure 5 (online colour at: www.pss-a.com) (a) Voltage–current (*V–I*) characteristic of a 350 nm wide wire at 50 mK under different magnetic fields. The field is applied perpendicular to the plane of the sample. The behaviour is hysteretic until the applied field reaches 20 mT. (b) Differential resistance extracted from the *V–I* curves. The resistance goes to zero when the applied field is below 100 mT.

wires. For the measurement of the *V–I* curves, we have used a standard four probe dc technique. No significant difference was observed from the critical temperature measured on the 'bulk' sample (≈2.5 K for this wafer) except for the case of the narrowest wire (below 100 nm wide, $T_c \approx 1.7$ K). This was seen for all our superconducting diamond thin films: the critical temperature of the wires were those of the bulk material except for the cases where the wire width is less that 100 nm. The *V–I* curves in panel (a) are hysteretic due to thermal effect: when the critical current is reached, Joule effect heats up the wire and the critical current measured when subsequently decreasing the current is thus much lower than the critical current measured when increasing the current [12, 13]; moreover, this 'retrapping' current is independent of the temperature of the refrigerator, as the actual temperature of the sample is then fixed by the dc current trough the wire.

The critical field of this sample was also measured by applying magnetic field in and out of plane of the sample. In Fig. 5a and b, the *V–I* characteristics and differential resistance for a 350 nm wide wire under different magnetic fields and at 50 mK is shown. The critical current decreases when the applied magnetic field is increased. Further, it is to be noted that the *V–I* characteristic is no more hysteretic once the field goes beyond 20 mT. In this case, the Joule heating becomes negligible due to the lowering of the critical current. The derivatives of the *V–I* characteristics were calculated and the differential resistance of the data is shown

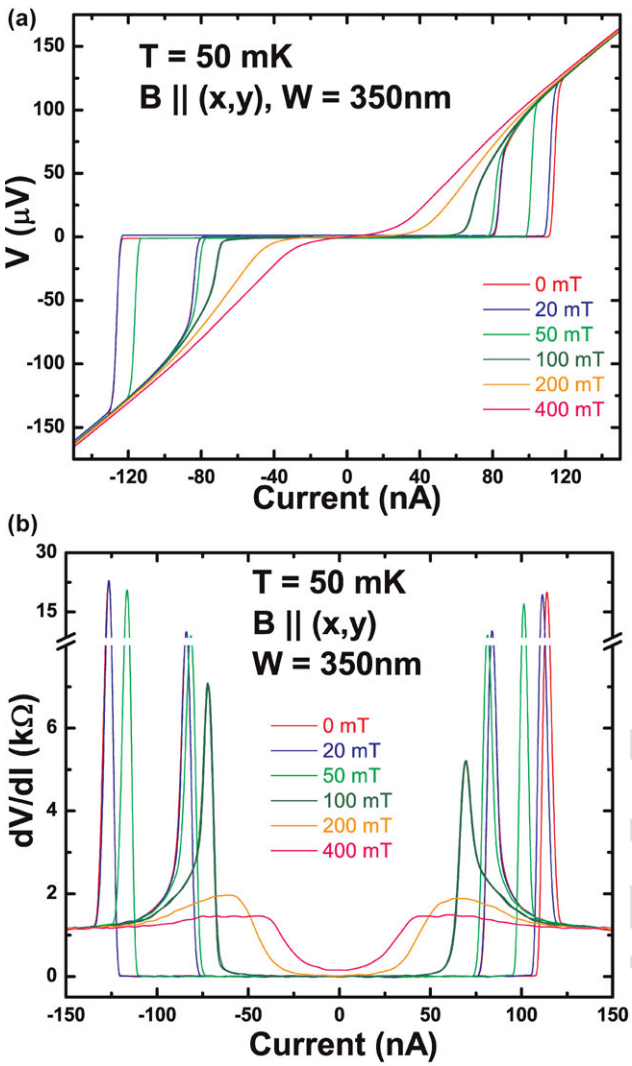

Figure 6 (online colour at: www.pss-a.com) (a) Voltage–current (V–I) characteristic of a 350 nm wide wire at 50 mK under different magnetic fields. The field is applied is in the plane of the sample. The behaviour is hysteretic until the applied field reaches 80 mT. (b) The differential resistance extracted from the V–I curves. The resistance goes to zero when the whole wire is in its superconducting state.

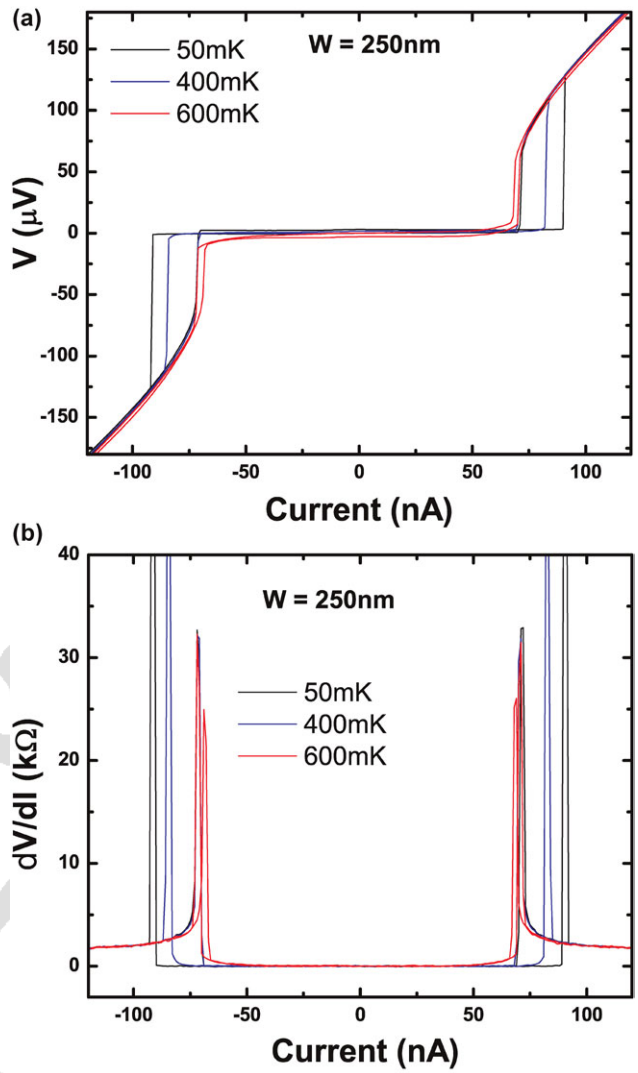

Figure 7 (online colour at: www.pss-a.com) (a) Voltage–current (V–I) characteristic of a 250 nm wide wire at different temperatures. The V–I curves are hysteretic due to thermal effect. (b) Differential resistance extracted from the V–I curves.

in Fig. 5b. One can see that when the applied field is smaller than 100 mT a clear zero is observed around $I = 0$. Now, when the field is increased further, a clear dip near the zero current even for applied fields as high as 2 T is seen. This shows that there are still pockets of superconductivity in the nanowires at such high fields. The most likely explanation would be that some grains in the wires remain superconducting even at such high magnetic field.

In Fig. 6a and b, the V–I characteristics and the differential resistance of the 350 nm wide wire when the applied field is in the plane of the sample and perpendicular to the current through the sample is shown. In this case, the hysteresis in the sample was completely removed only when the field was above 80 mT. So this means, that for the same applied field, the critical current is higher for the case when the applied field is in the plane of the sample. We do not have any definitive explanation to this effect but it is quite possible that the introduction of vortices plays a key role in the determination of the critical field. In this case, the difference in aspect ratio of the devices when applying the field perpendicular to the structures or in the plane of the structures may account for the observed behaviour. The differential resistance calculated for this configuration (shown in Fig. 6b) shows that there is distinct zero in the resistance even at fields as high as 200 mT.

In Fig. 7a and b, the V–I characteristics and the calculated differential resistance, respectively, are shown for a 250 nm wide and 500 nm long wire. The wire shows hysteresis due to

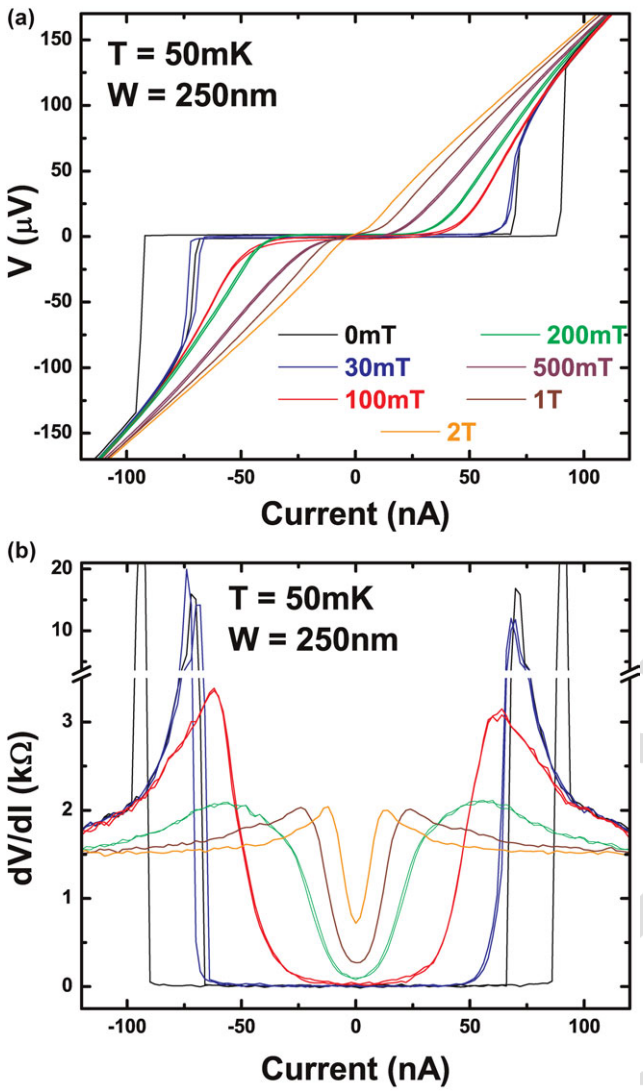

Figure 8 (online colour at: www.pss-a.com) (a) Voltage–current (V–I) characteristic of a 250 nm wide wire at 50 mK under different magnetic fields. The field is applied perpendicular to the plane of the sample. The behaviour is hysteretic until the applied field reaches 30 mT. (b) Differential resistance extracted from the V–I curves. The resistance goes to zero when the applied field is below 100 mT. The legends for this panel is same as that for (a).

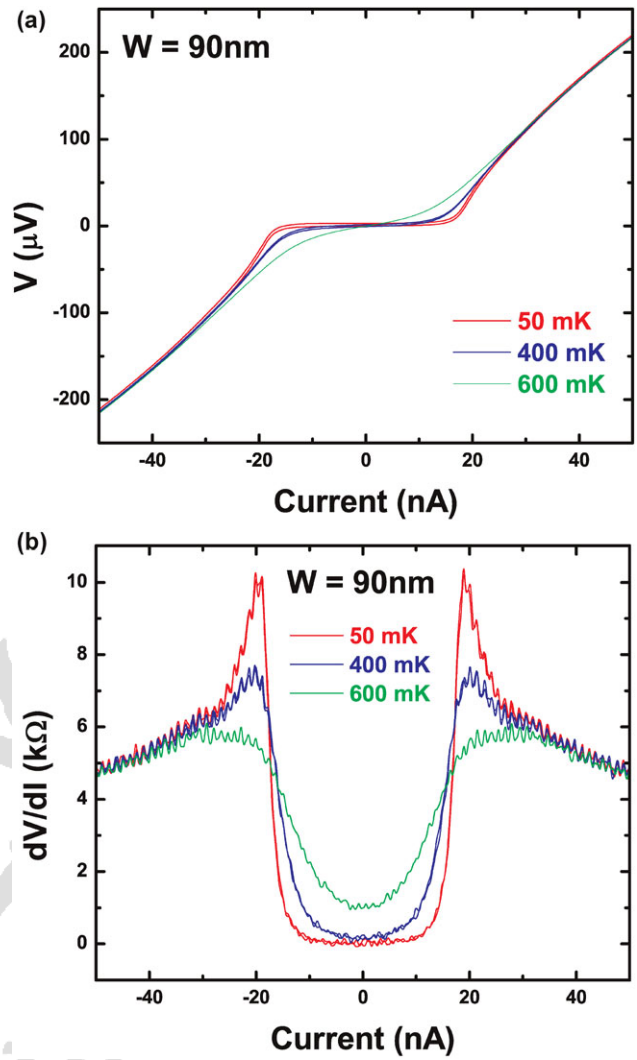

Figure 9 (online colour at: www.pss-a.com) (a) Voltage–current (V–I) characteristic of a 90 nm wide wire at different temperatures. (b) Differential resistance extracted from the V–I curves. The resistance goes to zero when the wire is in its superconducting state.

thermal effects until the temperature reaches 600 mK. The retrapping current in this case is of the order of 70 nA while for 350 nm wire it was 83 nA. If one defines the retrapping power as $I_r^2 R_r$, where I_r is the retrapping current and R_r is the retrapping resistance, then for a given sample this quantity should be constant. To check this fact with our experimental data, we compare the retrapping powers of two wires of different widths. Since in the nanowires presented in this paper the lengths and the thicknesses are constant one can say that the ratio of the widths of any two wires should be equal to the ratio of the squares of their respective retrapping currents. When one compares these ratio for the 350 and 250 nm wire, it is seen that the ratio of the widths is 1.4 which is similar to the ratio of the squares of the retrapping current for the corresponding wires. Hence, we can conclude that the retrapping power is an intrinsic property of the sample.

In Fig. 8a and b, the field dependence of critical current and differential resistance at a fixed temperature of 50 mK for the 250 nm wide wire is shown. One can see that the curves are hysteretic but the hysteresis disappears on applying a magnetic field of 30 mT. The differential resistance plotted in panel (b) of the same figure reveals the presence of few grains (as seen for 350 nm wide wire as well) having critical field above 2 T.

In Fig. 9a and b, the V–I characteristics and differential resistance respectively, of a 90 nm wide and 500 nm long wire as a function of temperature is shown. Here the

characteristic is not hysteretic. This can be explained as follows. The retrapping power for this sample is ~4.5 pW. For 90 nm wide wire, the power dissipated at the critical current at 50 mK is equal to 0.65 pW, which is much less than the retrapping power and hence the hysteretic behaviour is not seen. The differential resistance plotted in panel (b) shows that the sample is completely superconducting below 400 mK and above this temperature, the wire remains in the superconducting transition region until it reaches a temperature of ~1.7 K (inset of Fig. 4).

4 Conclusion In conclusion, nanostructures from boron-doped nanocrystalline superconducting diamond has been successfully fabricated. Using electron beam lithography, devices of characteristic size less that 100 nm and aspect ratio as high as 1:3 have been prepared. These structures have critical temperatures in the Kelvin range, similar to what is observed in 'bulk'; only a slight decrease of T_c is observed for wires thinner than 100 nm. Critical fields close to 100 mT were measured and traces of superconductivity were observed even under magnetic fields as strong as 2 T. The experiments also revealed that there is stronger suppression of critical properties when the applied magnetic field is perpendicular to the sample plane. This study proves that superconductivity in boron-doped diamond is a very robust phenomenon which makes it a promising candidate for future applications in the field of superconducting nanoelectro-mechanical systems.

Acknowledgements We thank L. Marty for help in the AFM measurements and P. Mohanty and M. Imboden for fruitful discussions. This work has been supported by the French National Agency (ANR) in the frame of its programme in 'Nanosciences and Nanotechnologies' (supernems project no. ANR-08-NANO-033).

Q1: Author: Please provide the keywords.

References

[1] J. Nagamatsu, N. Nakagawa, T. Muranaka, Y. Zenitani, and J. Akimitsu, Nature **410**, 63 (2001).
[2] E. A. Ekimov, V. A. Sidorov, E. D. Bauer, N. N. Mel'nik, N. J. Curro, J. D. Thompson, and S. M. Stishov, Nature **428**, 542 (2004).
[3] X. Blase, É. Bustarret, C. Chapelier, T. Klein, and C. Marcenat, Nature Mater. **8**, 375 (2009).
[4] G. A. Dubitskiy, V. D. Blank, S. G. Buga, E. E. Semenova, V. A. Kul'bachinskii, A. V. Krechetov, and V. G. Kytin, JETP Lett. **81**, 260 (2005).
[5] M. Nesládek, D. Tromson, C. Mer, P. Bergonzo, P. Hubik, and J. J. Mares, Appl. Phys. Lett. **88**, 232111 (2006).
[6] W. Gajewski, P. Achatz, O. A. Williams, K. Haenen, È. Bustarret, M. Stutzmann, and J. A. Garrido, Phys. Rev. B **79**, 045206 (2009).
[7] P. Achatz, W. Gajewski, É. Bustarret, C. Marcenat, R. Piquerel, C. Chapelier, T. Dubouchet, O. A. Williams, K. Haenen, J. A. Garrido, and M. Stutzmann, Phys. Rev. B **79**, 201203 (2009).
[8] M. Imboden, P. Mohanty, A. Gaidarzhy, J. Rankin, and B. W. Sheldon, Appl. Phys. Lett. **90**, 173502 (2007).
[9] O. A. Williams, O. Douhéret, M. Daenen, K. Haenen, E. Ōsawa, and M. Takahashi, Chem. Phys. Lett. **445**, 255 (2007).
[10] M. P. Villar, Ma. P. Alegre, D. Araujo, É. Bustarret, P. Achatz, L. Saminadayar, C. Bäuerle, and O. A. Williams, Phys. Status Solidi A **206**, 1986 (2009).
[11] M. Bernard, A. Deneuville, T. Lagarde, É. Treboux, J. Pelletier, P. Muret, N. Casanova, and É. Gheeraert, Diamond Relat. Mater. **11**, 828 (2002).
[12] W. Rabaud, L. Saminadayar, D. Mailly, K. Hasselbach, A. Benoît, and B. Étienne, Phys. Rev. Lett. **86**, 3124 (2001).
[13] H. Courtois, M. Meschke, J. T. Peltonen, and J. P. Pekola, Phys. Rev. Lett. **101**, 067002 (2008).

physica status solidi a
www.pss-a.com
applications and materials science

2010

WILEY-BLACKWELL
WILEY-VCH GmbH & Co. KGaA
physica status solidi
Rotherstrasse 21
10245 Berlin
Germany
TEL +49 (0) 30–47 03 13 31
FAX +49 (0) 30–47 03 13 34
E-MAIL pssa.proofs@wiley-vch.de

WILEY
Publishers Since 1807

Manuscript No.

Author/Title/Issue No.

Required Fields may be filled in using Acrobat Reader

Please correct your galley proofs and return them within 4 days together with the completed reprint order form. The editors reserve the right to publish your article with editors' corrections if your proofs do not arrive in time.

After having received your corrections, your paper will be published online up to several weeks ahead of the print edition in the EarlyView service of Wiley InterScience (www.interscience.wiley.com).
Please keep in mind that reading proofs is your responsibility. Corrections should therefore be clear. The use of standard proof correction marks is recommended. Corrections listed in an electronic file should be sorted by line numbers.
LaTeX and Word files are sometimes slightly modified by the production department to follow general presentation rules of the journal.

Note that the quality of the halftone figures is not as high as the final version that will appear in the issue.

Check the enclosed galley proofs very carefully, paying particular attention to the formulas (including line breakings introduced in production), figures, numerical values, tabulated data and layout of the pages.
A black box (■) or a question at the end of the paper (after the references) signals unclear or missing information that specifically requires **your attention.** Note that the author is liable for damages arising from incorrect statements, including misprints.

The main aim of proofreading is to correct errors that may have occurred during the production process, **and not to modify the content of the paper**. Corrections that may lead to a change in the page layout should be avoided.

Note that sending back a corrected **manuscript** file **is of no use**.

If your paper contains **color figures**, please fill in the Color Print Authorization and note the further information given on the following pages. Clearly mark desired **color print figures** in your proof corrections.

Return the corrected proofs within 4 days by e-mail.
Please do not send your corrections to the typesetter but to the Editorial Office.

E-MAIL: pssa.proofs@wiley-vch.de

Please limit corrections to errors in the text; cost incurred for any further changes or additions will be charged to the author, unless such changes have been agreed upon by the editor.

Full color reprints, PDF files, Issues, Color Print, and Cover Posters may be ordered by filling out the accompanying form.

Order Form

physica status solidi a
www.pss-a.com
applications and materials science

2010

WILEY-BLACKWELL
WILEY-VCH GmbH & Co. KGaA
physica status solidi
Rotherstrasse 21
10245 Berlin
Germany
TEL +49 (0) 30–47 03 13 31
FAX +49 (0) 30–47 03 13 34
E-MAIL pssa.proofs@wiley-vch.de

Please complete this form and return it by FAX or e-mail.

Manuscript No.

Author/Title/Issue No.

Required Fields may be filled in using Acrobat Reader

Reprints/Issues/PDF Files/Posters

Whole issues, reprints and PDF files (300 dpi) for an unlimited number of printouts are available at the rates given on the third page. Reprints and PDF files can be ordered before *and after* publication of an article. All reprints will be delivered in full color, regardless of black/white printing in the journal.

Reprints

Please send me and bill me for

full color reprints with color cover

full color reprints with color cover ***and*** customised color sheet

Issues

Please send me and bill me for

entire issues

PDF

Please send me and bill me for

❒ a PDF file (300 dpi) for an unlimited number of printouts **with customised cover sheet.**

The PDF file will be sent to your e-mail address.

Send PDF file to:

Please note that posting of the final published version on the open internet is not permitted. For author rights and re-use options, see the Copyright Transfer Agreement at http://www.wiley.com/go/ctavchglobal.

Cover Posters

Posters are available of all the published covers in two sizes (see attached price list). **Please send me and bill me for**

A2 (42 × 60 cm/17 × 24in) posters

A1 (60 × 84 cm/24 × 33in) posters

Mail reprints and/or issues and/or posters to (no P.O. Boxes):

Color print authorization

Please bill me for

color print figures (total number of color figures)

❒ YES, please print Figs. No. in color.

❒ NO, please print all color figures in black/white.

VAT number:

Tax-free charging can only be processed with the **VAT** number of the institute/company. To prevent delays, please provide us with the VAT number with this order.

Purchase Order No.:

Terms of payment:
☐ Please send an invoice ☐ Cheque is enclosed
Please charge my credit card

Expiry date

VISA ☐ MasterCard ☐ AMERICAN EXPRESS ☐

Card no.	
Card Verification Code	

Date, Signature _____

Send bill to:

Signature _____

Date _____

Subscriptions

For **subscriptions**, please send your order to:
WILEY-VCH Verlag GmbH & Co. KGaA, P.O. Box 101161, 69451 Weinheim, Germany.
Tel. + 49 (0) 62 01–60 64 00, Fax + 49 (0) 62 01–60 61 84, e-mail: subservice@wiley-vch.de or to a bookseller.

Price List for Reprints 2010 – pss (a)

WILEY
Publishers Since 1807

The prices listed below are valid only for orders received in the course of 2010. Minimum order is 50 copies.
Reprints can be ordered before *and after* publication of an article. All reprints are delivered with color cover and color figures. If more than 500 copies are ordered, special prices are available upon request.
Single issues are available to authors at a reduced price.
The prices include mailing and handling charges. All prices are subject to local VAT/sales tax.

Reprints with color cover	Price for orders of (in Euro)					
Size (pages)	50 copies	100 copies	150 copies	200 copies	300 copies	500 copies*
1– 4	314,—	367,—	425,—	445,—	548,—	752,—
5– 8	448,—	530,—	608,—	636,—	784,—	1077,—
9–12	581,—	683,—	786,—	824,—	1016,—	1396,—
13–16	708,—	832,—	958,—	1004,—	1237,—	1701,—
17–20	843,—	990,—	1138,—	1196,—	1489,—	2022,—
for every additional 4 pages	134,—	156,—	175,—	188,—	231,—	315,—
for additional customised colored cover sheet	**190,—**	**340,—**	**440,—**	**650,—**	**840,—**	**990,—**

PDF file (300 dpi, unlimited number of printouts, customised cover sheet)	€ 330.00
Issues	€ 48.00 per copy for up to 10 copies.*
Cover Posters	• A2 (42×60 cm/17×24in) € 49.00 • A1 (60×84 cm/24×33in) € 69.00

*Prices for more copies available on request.

Special offer: If you order 100 or more reprints you will receive a pdf file (300 dpi, unlimited number of printouts, color figures) and an issue for free.

Color figures

If your paper contains **color figures**, please notice that, generally, these figures will appear in color in the online PDF version and all reprints of your article at no cost. This will be indicated by a note „(online color at: www.pss-a.com)“ in the caption. The print version of the figures in the journal hardcopy will be black/white unless the author explicitely requests a color print publication and contributes to the additional printing costs.

	Approximate color print figure charges	
First figure	€ 495.00	
Each additional figure	€ 395.00	Special prices for more color print figures on request

If you wish color figures in print, please answer the **color print authorization** questions on the second page of our Order Form and clearly mark the desired color print figures in your proof corrections.

Information regarding VAT:

Please note that for German sales tax purposes the charge for *color print* is considered a service and therefore is subject to German Sales tax. For **institutional** customers in other countries the tax will be waived, i.e. the Recipient of Service is liable for VAT. Members of the EU will have to present a VAT identification number. Customers in other countries may also be asked to provide according tax identification information.